The Only Stable State of O_2^- Is the X $^2\Pi_g$ Ground State and It (Still!) Has an Adiabatic Electron Detachment Energy of 0.45 eV

Kent M. Ervin*,†

Department of Chemistry and Chemical Physics Program, University of Nevada, Reno, Nevada 89557

Iwona Anusiewicz,‡ Piotr Skurski,‡ and Jack Simons*,⊥

Department of Chemistry, University of Utah, 315 S. 1400 E., Rm 2020, Salt Lake City, Utah 84112

W. Carl Lineberger*,§

*JILA, University of Colorado and National Institute for Standards and Technology, and
Department of Chemistry and Biochemistry, University of Colorado, Boulder, Colorado 80309*

Received: June 18, 2003

The ultraviolet photoelectron spectrum of O_2^- exhibits 29 resolved vibronic transitions to the three low-lying electronic states of neutral O_2 (X $^3\Sigma_g^-$, a $^1\Delta g$, b $^1\Sigma_g^+$) from the X $^2\Pi_J$ ($J = 3/2$ and 1/2) spin−orbit states of the anion. A Franck−Condon simulation, using the established molecular constants of the neutral oxygen states, matches every observed feature in the spectrum. The 0−0 origin transition is unambiguously assigned, yielding the electron affinity $EA_0(O_2) = 0.448 \pm 0.006$ eV. The derived bond dissociation energy is $D_0(O_2^-)$ = 395.9 ± 0.6 kJ/mol. Coupled-cluster theory at the CCSD(T)/aug-cc-pVTZ level is used to determine the potential energy curves of O_2 and of O_2^- in its ground state and two excited states, in both the electronically bound and unbound regions. Stabilization methods are employed to characterize the anion curves at bond lengths where their electronic energies lie above that of the ground-state neutral. The calculations confirm that the O_2^- X $^2\Pi_g$ ground state is adiabatically stable, but the lowest electronically excited states of O_2^- (a $^4\Sigma_u^-$ and A $^2\Pi_u$) are adiabatically unbound with respect to electron detachment. The calculations predict the anionic doublet−quartet splitting to be $T_e(a\ ^4\Sigma_u^-) - T_e(X\ ^2\Pi_g) = 2.40$ eV and the first excited doublet at an energy of $T_e(A\ ^2\Pi_u) - T_e(X\ ^2\Pi_g) = 3.39$ eV. These observations are consistent with electron scattering on O_2 and other experimental data, and they sharply refute recent interpretations of electron-capture detector experiments that $EA(O_2) \approx 1$ eV, that O_2^- has multiple excited states below the neutral ground-state minimum, and that the doublet−quartet splitting is 0.12 eV [Chen, E. S.; Chen, E. C. M. *J. Phys. Chem. A* **2003,** *107,* 169.].

Introduction

The gas-phase O_2^- molecular anion is important in the chemistry of the upper atmosphere[1] and superoxides are essential in biological systems, mediating enzymatic triplet-to-singlet oxygen activation.[2] The stability of the O_2^- ion, as measured by the adiabatic electron affinity of oxygen, $EA_0(O_2)$, is therefore of great practical and fundamental interest. Early measurements and estimates varied widely (Table 1),[3−9] so it is not surprising that O_2^- was one of the first molecular anions investigated by negative-ion laser photoelectron spectroscopy (PES) in 1972.[10] Celotta et al.[10] observed transitions from mass-selected O_2^- to vibrational levels of the X $^3\Sigma_g^-$ and a $^1\Delta_g$ states of O_2, assigned the spectrum on the basis of the known molecular constants of the neutral, and obtained[10] $EA_0(O_2) = 0.436 \pm 0.008$ eV. Since then, the photoelectron spectrum of O_2^- has been observed using a variety of ion sources, laser wavelengths, and types of photoelectron spectrometers.[11−20] Technological improvements in the resolution of photoelectron spectrometers have resulted

in modest revision of the 1972 value—Ellison and co-workers[12] reported $EA_0(O_2) = 0.451 \pm 0.007$ eV and Shiedt and Weinkauf[19] reported $EA_0(O_2) = 0.450 \pm 0.002$ eV. Most of the determinations by other methods since the early 1970s, as compared in Table 1,[3,21−33] agree with these PES values.

The valence molecular orbital configurations of the lowest electronic states of O_2^- are as follows.

$$X\ ^2\Pi_g\ (2s\sigma_g)^2(2s\sigma_u^*)^2(2p\sigma_g)^2(2p\pi_u)^4(2p\pi_g^*)^3$$

$$a\ ^4\Sigma_u^-\ (2s\sigma_g)^2(2s\sigma_u^*)^2(2p\sigma_g)^2(2p\pi_u)^4(2p\pi_g^*)^2(2p\sigma_u^*)^1$$

$$A\ ^2\Pi_u\ (2s\sigma_g)^2(2s\sigma_u^*)^2(2p\sigma_g)^2(2p\pi_u)^3(2p\pi_g^*)^4$$
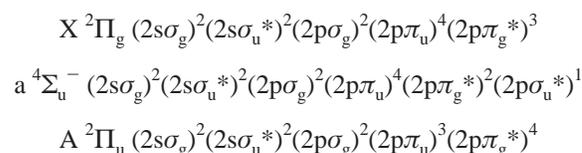
The X $^2\Pi_g$ ground electronic state of O_2^- has a bond order of 1.5 and it is the only electronic term that arises from this optimal molecular orbital configuration. Formation of any valence excited state requires an electron promotion, either from a bonding orbital to an antibonding orbital, or from the antibonding $2p\pi_g^*$ orbital to the more strongly antibonding $2p\sigma_u^*$ orbital. The A $^2\Pi_u$ state was observed for O_2^- dissolved in alkali crystal salts, with an electronic term energy of 3.4 eV above the ground state and an estimated 0.45 Å expansion of the internuclear distance,[34,35] consistent with its lower bond order of 0.5. In the

* To whom correspondence should be addressed.

† E-mail: ervin@chem.unr.edu.

‡ Also Department of Chemistry, University of Gdansk, Sobieskiego 18, 80-952 Gdansk, Poland.

⊥ E-mail: simons@chem.utah.edu.

§ E-mail: wcl@jila.colorado.edu.

TABLE 1: Comparison of Experimental Electron Affinities of O$_2$

EA$_0$(O$_2$)^a/eV	method^b	year	ref
0.448 ± 0.006	PES	2003	this work
1.07 ± 0.07	ECD	2003	Chen and Chen[42,43]
0.9 ± 0.05	ECD	2002	Chen et al.[41]
0.444 ± 0.03	ES	1995	Allan[21]
0.450 ± 0.002	PES	1995	Schiedt and Weinkauf[19]
0.451 ± 0.007	PES	1989	Travers et al.[12]
0.43 ± 0.03	ES	1986	Stephen and Burrow[22]
0.46 ± 0.05	ECD	1983	Chen and Wentworth[23]
0.44 ± 0.1	CID	1978	Tiernan and Wu[24]
0.4 ± 0.1	NBIE	1977	Durup et al.[25]
0.45 ± 0.025	ES	1974	Burrow[26]
0.5	ECD	1972	Van de Wiel and Tommassen[28]
0.5 ± 0.1	NBIE	1972	Baeda[27]
0.436 ± 0.008	PES	1972	Celotta et al.[10,c]
>0.45 ± 0.1	endo	1971	Tiernan et al.[29]
>0.48	endo	1971	Berkowitz et al.[30]
>0.56 ± 0.10	endo	1971	Chantry[31]
0.46 ± 0.05	NBIE	1971	Nalley and Compton[32]
0.5 ± 0.2	endo	1970	Lacmann & Herschbach[33]
<0.77, >0.78, >1.13 eV	IMRB	1970	Vogt et al.[5,c]
>1.27 ± 0.20	endo	1970	Bailey and Mahadevan[4]
>1.1 ± 0.1	AE	1969	Stockdale et al.[6]
0.43 ± 0.02	swarm	1966	Pack and Phelps[7]
0.46 ± 0.02	swarm	1961	Phelps and Pack[8]
0.15 ± 0.05	PD	1958	Burch et al.[9]

^{a} Experimental values from the NIST compilation[3] with some additions and minor corrections. ^{b} PES, photoelectron spectroscopy; ECD, electron-capture detector; ES, electron scattering; CID, collision-induced dissociation; NBIE, neutral beam ionization; swarm, electron swarm attachment/detachment kinetics; endo, endothermic reaction threshold; IMRB, ion−molecule reaction bracketing; AE, electron ionization apperance energy; PD, photodetachment (threshold extrapolation). ^{c} Revised from original reference on the basis of current electron affinities of reference compounds.[3]

gas phase, the O$_2^-$ A $^2\Pi_u$ state is implicated in dissociative attachment[36] of electrons to O$_2$ via a Feshbach resonance yielding O$^-$ + O and is also observed as resonances in electron scattering.[37,38] Johnson and co-workers[14,16] identified the A $^2\Pi_u$ resonance state in gas-phase O$_2^-$ by photofragmentation spectroscopy[14] and via non-Franck−Condon vibronic intensities in the photoelectron spectrum[16] at a photon energy of 3.969 eV. These observations place the A $^2\Pi_u$ state well above the O$_2$ + e$^-$ detachment limit. Electron scattering on O$_2$ at higher energies, 4−15 eV, shows resonances involving the repulsive parts of the $^4\Sigma_u^-$ and $^2\Sigma_u^-$ potential curves of O$_2^-$ imbedded in the O$_2$ + e$^-$ continuum.[37] Phosphorescence from O$_2^-$ in a quartet excited state has been seen from superoxide defects in calcium oxide,[39] but to our knowledge gas-phase O$_2^-$ (a $^4\Sigma_u^-$) has not been observed spectroscopically. Theoretical calculations at the multiconfigurational SCF level[40] predict that the O$_2^-$ a $^4\Sigma_u^-$ quartet state has an excitation energy of 2.5−2.8 eV, also well above the detachment limit.[40]

Contrary to these results, Chen et al.[41−43] have recently reported an electron affinity of EA(O$_2$) = 1.07 ± 0.07 eV and an O$_2^-$ doublet−quartet splitting of 0.12 eV on the basis of electron-capture detector (ECD) method experiments and reassignments of the published photoelectron spectra. Chen and Chen[43] propose that 12 of the 24 possible electronic states of O$_2^-$ arising from O(^{3}P) + O$^-$(^{2}P) have minima with r_e = 1.29−1.40 Å that lie below the O$_2$ + e$^-$ ground-state minimum. Here, we present vibrational and spin−orbit state-resolved ultraviolet photoelectron spectra and high-level ab initio quantum mechanical calculations that show unequivocally that these assignments[41−43] of a high electron affinity and of multiple adiabatically electronically bound O$_2^-$ excited states are incorrect. Our results may be compared with previous photoelectron spectroscopy[11−20] and electron scattering[21,22,36−38,44−49] experiments and theoretical calculations.[40,50−57]

Photoelectron Spectroscopy of O$_2^-$. *Experimental Methods.* The negative ion photoelectron spectrometer used in this work has been described in detail.[17,58,59] Negative ions are formed in a microwave discharge flowing afterglow source in a helium buffer gas at 0.8 Torr. The ions are extracted from the flow tube, focused, accelerated into a Wien velocity filter for mass selection, and decelerated to 40 eV before entering the laser interaction region. An argon ion laser operated at 363.8 nm ($h\nu$ = 3.408 eV) provides the ultraviolet radiation, amplified in an external power buildup cavity surrounding the interaction zone. The electron kinetic energy (eKE) is measured using a hemispherical electrostatic energy analyzer and a position-sensitive detector. The electron binding energies (eBE) are given by eBE = $h\nu$ − eKE.

The electron binding energy scale is calibrated on the atomic transitions O(^{3}P$_{J'}$) ← O$^-$(^{2}P$_{J''}$), P(^{4}S$_{3/2}$) ← P$^-$(^{3}P$_{J''}$), and P(^{2}D$_{J'}$) ← P$^-$(^{3}P$_{J''}$), using EA$_0$(O) = 1.46111$_2$ eV,[60−63] EA$_0$(P) = 0.7465 ± 0.0003 eV,[61,64] and the P(^{4}S$_{3/2}$ ← ^{2}D$_{3/2}$) energy level spacing[65] of 11361.02 cm^{-1}. The oxygen ions were produced from O$_2$ added upstream of the microwave discharge. The phosphorus anions were produced from phosphine (caution−toxicity hazard) leaked into the flow tube downstream of the discharge, with the oxygen flow turned off. The oxygen and phosphorus atomic spectra were measured immediately before and after the O$_2^-$ spectrum, respectively. A linear compression factor[58] for the relative energy scale of 0.5 ± 0.2% is determined from the spacing of the phosphorus transitions. The instrumental resolution function is obtained by fitting the atomic oxygen O(^{3}P$_{J'}$) ← O$^-$(^{2}P$_{J''}$) transitions as shown in Figure 1.[61,65−67] The resolution function from the fit is a Gaussian distribution with a 6 meV full width at half-maximum (fwhm) atop a second Gaussian "pedestal" of 25 meV fwhm and 6% relative intensity.

Figure 1. Photoelectron spectrum of O$^-$ as a function of electron binding energy (lower axis) and electron kinetic energy (upper axis) at a laser wavelength of 364 nm ($h\nu$ = 3.408 eV). The solid circles are experimental points. The solid line is a fit using the instrumental resolution function (peak shape) shown in the inset (6-meV fwhm Gaussian plus a second 25-meV fwhm Gaussian "pedestal" at 6% relative intensity). The energies of spin−orbit transitions, labeled at the top of the plot, are set to the known values.[61,65] The open bars (left side) represent the intensities obtained from the least-squares fit. The solid bars (right side) represent the theoretical relative intensities calculated using L−S coupling and assuming p-electron detachment.[67]

Figure 2. (a) Photoelectron spectrum of O_2^- as a function of electron binding energy (lower axis) and electron kinetic energy (upper axis) at a laser wavelength of 364 nm ($h\nu = 3.408$ eV). The combs above the spectrum identify $v' \leftarrow v''$ vibrational assignments for transitions from the X $^2\Pi_g$ ground state of O_2^- to three electronic states of neutral O_2 (X $^3\Sigma_g^-$, a $^1\Delta_g$, and b $^1\Sigma_g^+$). Peak positions are calculated using the molecular constants in Table 2. Each transition is a doublet. The larger (left) peak arises from the lower X $^2\Pi_{3/2}$ spin−orbit state of the anion and the smaller (right) peak arises from the excited X $^2\Pi_{1/2}$ state. (b) Franck−Condon simulation of the spectrum as described in the text. The inset shows the rotational and spin−orbit contour of the doublet peaks, calculated as described in the text.

TABLE 2: Experimental Spectroscopic Constants of O_2^- and O_2

quantity	O_2^- X $^2\Pi_g$	O_2 X $^3\Sigma_g^-$	O_2 a $^1\Delta_g$	O_2 b $^1\Sigma_g^+$
r_e/Å	1.348 ± 0.008	1.2075	1.2155	1.2268
B_e/cm^{-1}	1.161 ± 0.007	1.4457	1.4264	1.4004
ω_e/cm^{-1}	1108 ± 20	1580.1	1509.8	1432.7
$\omega_e x_e$/cm^{-1}	[9][a]	11.9	13.1	13.9
ν_{01}/cm^{-1}	1090 ± 20	1556.3	1483.6	1404.9
A/cm^{-1}	-153 ± 11[b]			
T_0/eV	0	0	0.9773	1.6268
T_e/eV	0	0	0.9817	1.6360
$EA_0(O_2)$/eV	0.448 ± 0.006			
$EA_e(O_2)$ /eV	0.409 ± 0.006[c]			
refs	this work	68, 69	68, 70, 72	68, 71, 73

[a] Estimated for a Morse potential using $D_0(O_2^-)$ from Table 4 (see text). [b] Spin−orbit coupling constant, $A = -\Delta_{so} - 2B''$ (ref 74). [c] $EA_e = EA_0 + \omega_e''/2 - \omega_e x_e''/4 - \omega_e'/2 + \omega_e x_e'/4 + A/2$.

Spectral Assignments. The ultraviolet photoelectron spectrum of O_2^- is displayed in Figure 2a. A preliminary spectrum was presented previously without detailed calibration or analysis.[17] Figure 2 shows the assignments of the vibronic transitions from the $v'' = 0$, 1, and 2 vibrational states of the $^2\Pi_{3/2}$ and $^2\Pi_{1/2}$ spin−orbit states of the anion to the v' vibrational states of the three low-lying electronic states of O_2 (X $^3\Sigma_g^-$, a $^1\Delta_g$, and b $^1\Sigma_g^+$). No unassigned transitions are observed. The energy levels of neutral oxygen are calculated from the established spectroscopic constants collected in Table 2.[68–74] Experimental and calculated peak positions for 29 observed lines are listed in Table 3. The excellent match of the known energy levels of O_2 with the observed peak positions (mean absolute error 0.9 meV) confirms the identity of the 32-amu ion as O_2^-. The vibrationless

origin transition, O_2 X $^3\Sigma_g^-$ ($v' = 0$) $\leftarrow$ O_2^- X $^2\Pi_{3/2}$ ($v'' = 0$), at eBE ≈ 0.45 eV is unambiguously assigned by the difference between the vibrational spacings of the neutral ground state (ν_{01}' = 1556.3 cm^{-1} from Table 2) and of the anion (ν_{01}'' = 1090 ± 20 cm^{-1} observed hot band). The observed anion fundamental frequency ν_{01}'' agrees with previous measurements of 1073 ± 50 cm^{-1} from photoelectron spectroscopy,[12] 1078−1081 cm^{-1} from high-resolution electron scattering resonances,[21,22,44] 1090 cm^{-1} extrapolated from Raman spectra of O_2^- in alkali halide salts,[75] and 1084 ± 6 cm^{-1} from A−X band autodetachment resonances.[16]

A variety of ion sources have been used for acquiring O_2^- spectra, including flowing afterglow (this work), high-pressure discharges,[10,12] pulsed-beam supersonic jets,[13–16,18–20] and

8524 *J. Phys. Chem. A, Vol. 107, No. 41, 2003*

Ervin et al.

TABLE 3: Peak Positions and Assignments

assignment[a]	eBE (exp)[b]/eV	eBE (calc)[c]/eV	error/eV
b(4)−X(0)	(2.7487)	2.7509	0.0022
b(3)−X(0)	2.5816	2.5870	0.0054
b(2)−X(0)	2.4173	2.4197	0.0024
a(5)−X(0)	2.3131	2.3125	−0.0006
b(1)−X(0)	2.2484	2.2490	0.0006
a(4)−X(0)	2.1421	2.1416	−0.0005
b(0)−X(0)	2.0720	2.0748	0.0028
a(3)−X(0)	1.9671	1.9674	0.0003
a(2)−X(0)	1.7898	1.7899	0.0001
a(1)−X(0)	1.6093	1.6092	−0.0001
X(6)−X(0)	1.5612	1.5615	0.0003
a(1)−X(1)	1.4736	1.4741	0.0005
a(0)−X(0)	1.4262	1.4253	−0.0009
X(5)−X(0)	1.3832	1.3833	0.0001
a(0)−X(1)	1.2915	1.2902	−0.0013
X(5)−X(1)	1.2471	1.2481	0.0010
X(4)−X(0)	1.2021	1.2021	0.0000
X(4)−X(1)	1.0677	1.0670	−0.0007
X(3)−X(0)	1.0186	1.0180	−0.0006
X(4)−X(2)	(0.9329)	0.9341	0.0012
X(2)−X(0)	0.8318	0.8310	−0.0008
X(3)−X(2)	(0.7500)	0.7500	0.0000
X(2)−X(1)	(0.6968)	0.6958	−0.0010
X(1)−X(0)	0.6412	0.6410	−0.0002
X(1)−X(1)	0.5058	0.5058	0.0000
X(0)−X(0)	0.4482	0.448	−0.0002
X(1)−X(2)	(0.3709)	0.3729	0.0020
X(0)−X(1)	0.3132	0.3129	−0.0003
X(0)−X(2)	(0.1795)	0.1799	0.0004

[a] Primary assignment. [b] Electron binding energies of peak positions fit using the rotational contour described in the text. Weak transitions in parentheses. [c] eBE = $EA_0(O_2) + T_0(O_2) + \omega_e'(v') - \omega_e x_e'(v')(v' + 1) - \omega_e''(v'') + \omega_e x_e''(v'')(v' + 1)$, using constants from Table 2.

cesium-ion sputtering.[11] The position of the assigned origin transition, eBE ≈ 0.45 eV, is invariant in all of these published photoelectron spectra. The observation that all of these ion sources produce the same electronic state of O_2^-, and no others, indicates that it is the ground electronic state. Vibrational states of O_2^- up to $v'' = 3$ have been observed as hot bands in photoelectron spectra,[11,19,20] while higher vibrational states, $v'' \geq 4$, are above the detachment limit and have been observed as resonances in low-energy electron scattering on O_2.[22,44−49] The hot bands are further identified by their different intensities relative to the origin in previously published photoelectron spectra with different O_2^- vibrational temperatures. For example, intense $v'' = 1$, 2, and 3 hot bands at eBE ≈ 0.31, 0.18, and 0.05 eV, respectively, are observed from a hot cesium-ion sputtering source,[11] while they are absent from a cold pulsed-beam supersonic jet source.[13]

The observation of both the singlet and triplet electronic states of O_2 identifies the anion as a doublet state (selection rule $\Delta S = \pm^1/_2$ for photodetachment). Two adjacent peaks are observed for each vibronic transition for all three neutral electron states, indicating that the second peak arises from a common excitation in the anion. The $\Delta\Lambda = 0, \pm 1$ selection rule and the magnitude of the splitting identify the doublets as arising from the ground $^2\Pi_{3/2}$ state for the stronger peaks and the excited $^2\Pi_{1/2}$ spin−orbit state for the weaker peaks at lower electron binding energy. From peak fits of the doublets of the seven most intense vibronic transitions, the spin−orbit splitting is obtained as $\Delta_{so} = 18.7 \pm 1.3$ meV or 151 ± 11 cm^{-1}. This agrees with the value of 161 ± 4 cm^{-1} reported previously from photoelectron spectroscopy[19] and electron scattering measurements of 160 ± 16 cm^{-1},[48] and 160 ± 8 cm^{-1},[22] and 149 ± 8 cm^{-1}.[44]

No transitions are observed that could be assigned to electronically excited states of O_2^-. If the a $^4\Sigma_u^-$ quartet state

were present in the ion beam, transitions to the O_2 X $^3\Sigma_g^-$ neutral ground triplet state would be allowed but transitions to the O_2 a $^1\Delta_g$ and b $^1\Sigma_g^+$ excited singlet states would be forbidden by spin selection rules. The absence of unassigned transitions, particularly for the hotter ion sources used in previous PES work,[11] implies that low-lying (<0.45 eV) electronically excited states of O_2^- do not exist.

Franck−Condon Simulation. The spectroscopic assignments are further confirmed by a Franck−Condon simulation[66,76] of the transition intensities, shown in Figure 2b. The Franck−Condon factors are calculated by numerical integration of the overlaps between the Laguerre polynomial wave functions for Morse oscillator vibrational states.[77−79] The harmonic frequencies (ω_e'), anharmonicities ($\omega_e x_e'$), and bond lengths (r_e') of the three neutral O_2 electronic states are fixed at the literature values in Table 2. The 0−0 electron binding energies, harmonic frequency (ω_e''), bond length (r_e''), and vibrational populations of the anion are determined by least-squares fits to the data. The $v'' > 1$ hot band transitions are too weak to determine the anion anharmonicity reliably. Therefore, $\omega_e x_e'' = 9$ cm^{-1} is estimated from the Morse potential and the O_2^- dissociation energy. This value is consistent with values of 8 ± 2 cm^{-1} obtained from the O_2^- ($v'' \geq 4$) vibrational resonances observed in high-resolution electron scattering,[21,22,44] 8.5−8.8 cm^{-1} for O_2^- dissolved in alkali halides,[34] and values for isoelectronic species, 9.9 cm^{-1} for FO[80] and 9.8 cm^{-1} for F_2^+.[81]

The peak shapes are asymmetric because of unresolved rotational contours. To simulate the contour, rotational line positions and line strengths are calculated for $[O_2(^{1,3}\Sigma) + e^-] \leftarrow O_2^-(^2\Pi_g)$ and $[O_2(^1\Delta) + e^-] \leftarrow O_2^-(^2\Pi_g)$ adsorption transitions using the DIATOMIC program[82] with the rotational and spin−orbit coupling constants in Table 2. The stick spectra are convoluted by the instrumental resolution function described above, resulting in the contour in the inset of Figure 2b. The anion rotational and spin−orbit temperature is 400 ± 50 K, as roughly determined by matching the observed contours. The calculated contours for the three separate electronic bands are indistinguishable on the scale of Figure 2. The peak intensities are shifted by -2 ± 1 meV from the 0 K origin. This rotational shift is included automatically in the Franck−Condon analysis by using the calculated peak profile in the fits to the data.

Each of the three electronic bands are fit independently, but the final simulation in Figure 2b and the calculated peak positions in Table 3 use the averaged anion constants in Table 2. The anion frequency is fixed from the fit to the X−X band because hot band transitions are weak for the a−X and b−X bands. The $v'' = 1$ and $v'' = 2$ populations are non-Boltzmann, with effective vibrational temperatures of ~750 K and ~900 K, respectively. Electron attachment to O_2 in the discharge source produces vibrationally excited O_2^-, which may be inefficiently quenched by collisions with helium because of its high frequency. A similar vibrational temperature of 800 K was observed in the photoelectron spectrum[83] of FO$^-$. Independent fits to the three electronic states give electron affinities within 2 meV, using the known neutral term energies in Table 2 to correct to the ground-state origin. As a final check of the electron energy scale, the compression factor was recalculated using the energy levels of neutral O_2 as an internal calibration instead of the phosphorus calibration. The resulting electronic term energies are within 1 meV of the original calibration. The error limits reported in Table 2 are approximately ±2 combined standard uncertainties[84] and reflect the reproducibility among the three states, calibration uncertainty, temperature uncertainty, and statistical fitting error.

TABLE 4: Recommended Thermochemical Values

quantity	value/eV	value/kJ mol^{-1}	method	ref
EA$_0$(O$_2$)	0.448 ± 0.006	43.2 ± 0.6	photoelectron spectroscopy	this work
EA$_0$(O)	1.46111$_2$	140.976	photodetachment threshold	60−63
D$_0$(O$_2$)	5.11665 ± 0.00014	498.682 ± 0.014	spectroscopic	87
D$_0$(O$_2^-$)	4.104 ± 0.006	395.9 ± 0.6	D$_0$(O$_2$) − EA$_0$(O) + EA$_0$(O$_2$)	
D$_{298}$(O$_2^-$)		399.9 ± 0.7	D$_0$(O$_2^-$) + $\int_0^{298}\Delta_r C_p\,dT$	a
$\Delta_f H_{298}$(O$_2^-$)		−36.3 ± 0.7	−EA$_0$(O$_2$) + $\int_0^{298}\Delta_f C_p\,dT$	a,b

a Integrated heat capacities taken from Gurvich et al.[85]   *b* "Electron convention."[86]

The simulated spectrum is an excellent match of the observed spectrum (Figure 2), for both line positions and relative intensities. The transitions in the X−X band from $v'' = 1$ exhibit the characteristic double maximum in intensities at $v' = 1$ and 5 and a minimum at $v' = 3$ resulting from the node in the lower state vibrational wave function. This behavior definitively identifies the hot band as vibrational rather than an excited electronic state of O$_2^-$.

Electron Affinity and Related Thermochemistry. The final value of the electron affinity from the simulation is EA$_0$(O$_2$) = 0.448 ± 0.006 eV. The error bars overlap with the previous photoelectron spectrometry electron affinities of 0.450 ± 0.002 eV,[19] 0.451 ± 0.007 eV,[12] and 0.436 ± 0.008 eV.[10] The (small) spread in these values is largely due to different methods of estimating the rotational and spin−orbit corrections and the uncertainties of estimating the rotational and spin−orbit temperatures. The electron affinity from photoelectron spectroscopy is also in good accord with electron scattering and other independent experiments in the last three decades (other than the recent ECD results), as summarized in Table 1.

Additional thermochemical results and derivations are presented in Table 4.[85,86] Our experimental electron affinity of O$_2$ may be combined with the neutral dissociation energy[87] and the atomic oxygen electron affinity to obtain the dissociation energy, D_0(O$_2^-$) = 4.104 ± 0.006 eV. This value agrees with the prompt O$_2^-$ → O + O$^-$ photodissociation threshold near 4.09 eV observed by Johnson and co-workers[14,16] and the O$_2^-$ collision-induced dissociation threshold energy of 4.1 ± 0.1 eV reported by Tiernan and Wu.[24] The internal consistency of the thermochemical cycle for these independent experiments verifies the electron affinity value.

Theoretical Treatment of Potential Energy Curves of O$_2^-$ Electronic States. Modern electronic structure theory is capable of calculating electron affinities to a high degree of accuracy for small stable anions.[53,88−91] However, calculation of the potential energy curves of electronically unbound anion states is more challenging. Such states correspond to temporary anions (i.e., metastable electronic states) that can be observed as resonances in electron scattering and photodetachment experiments, and thus are also important to characterize. In the present study, all of the anion states we focus on are electronically unstable at some internuclear distances (R) and stable at others, so it is important to employ theoretical methods that allow us to describe the corresponding potential curves at all R-values.

The use of straightforward variational ab initio techniques for electronically unstable states with extremely large basis sets fails. Such approaches generate a wave function describing the neutral molecule plus a free electron infinitely distant and with essentially zero kinetic energy. This happens because the molecule-plus-free-electron function is indeed the lowest-energy solution to the Schrödinger equation in such cases; of course, it is not the solution we seek when we attempt to describe metastable resonance states of anions. The function we want is embedded within the continuum of molecule-plus-free-electron

functions. Using smaller basis sets cannot easily avoid these difficulties; instead, one must employ an approach that is designed to handle the metastability of such states.

In the so-called stabilization method,[92−95] one adds to the Hamiltonian H describing the system of interest a potential V that confines the extra electron to the molecular framework (i.e., does not allow it to escape). One then carries out a series of calculations on the anion using $H + \lambda V$ as the Hamiltonian (using values of λ for which the electronic state of interest is bound) and determining the energy of the desired anion state for a range of λ values. Because the energies of the neutral states are also usually altered when the Hamiltonian is replaced by $H + \lambda V$, one must also compute their energies at various λ values. By then extrapolating the anion and neutral state energies to $\lambda = 0$, one obtains the stabilization estimate for these energies.

In the particular variant of the stabilization method used here to obtain the resonance-state energies for O$_2^-$, we artificially increase the nuclear charge of each oxygen atom by an amount Δq to render the anionic state electronically bound and thus amenable to conventional ab initio treatment. These calculations are performed for several values of Δq and the energies are then extrapolated to $\Delta q = 0$ to obtain the true energy of the anion. To illustrate, we show plots of the Δq dependence of the anion−neutral energy differences associated with the ground state of the neutral and the X $^2\Pi_g$, a $^4\Sigma_u^-$, and A $^2\Pi_u$ states of the anion at $R = 1.313$ Å in Figure 3a and at $R = 1.813$ Å in Figure 3b. We plot the detachment energies (computed at the coupled-cluster single and double excitation with noniterative triple excitation level[96] using aug-cc-pVTZ basis functions[97]), which we label $D^{CCSD(T)}$. All of these calculations were performed using the Gaussian 98[98] suite of programs. The plots of $D^{CCSD(T)}$ versus Δq exhibit significant curvature and therefore the extrapolations employ quadratic fits. Plots of detachment energies rather than the anion and neutral total energies are used because such plots are more easily fit to a quadratic function of Δq and thus more efficiently extrapolated. The quality of the quadratic fits is high, with statistical r-values of 0.9964 or greater in all cases. At $R = 1.313$ Å, the X $^2\Pi_g$ state of the anion is bound (i.e., has a positive detachment energy), but the a $^4\Sigma_u^-$ and A $^2\Pi_u$ states are not. The plots for the a $^4\Sigma_u^-$ and A $^2\Pi_u$ states do not contain data points at $\Delta q = 0.1$ because at $\Delta q = 0.1$ these states have energies lying above that of the neutral ($D^{CCSD(T)} < 0$) and thus are inappropriate to include in the stabilization plots. In contrast, Figure 3b shows that at $R = 1.813$ Å, all three anion states are electronically bound, that is, the curves lie below the ground-state neutral O$_2$ curve at that internuclear distance. Finally, both parts of Figure 3 illustrate that the limits to the precision in the $D^{CCSD(T)}$ values obtained in the extrapolation are usually well within 0.1 eV. For the a $^4\Sigma_u^-$ state in regions where it is electronically unstable, we find the plots of $D^{CCSD(T)}$ versus Δq to have considerable quadratic character. Moreover, these plots often do not include values of Δq below 0.2 as explained above, and thus must be extrapolated over a longer range. Hence, our $D^{CCSD(T)}$ data for the a $^4\Sigma_u^-$
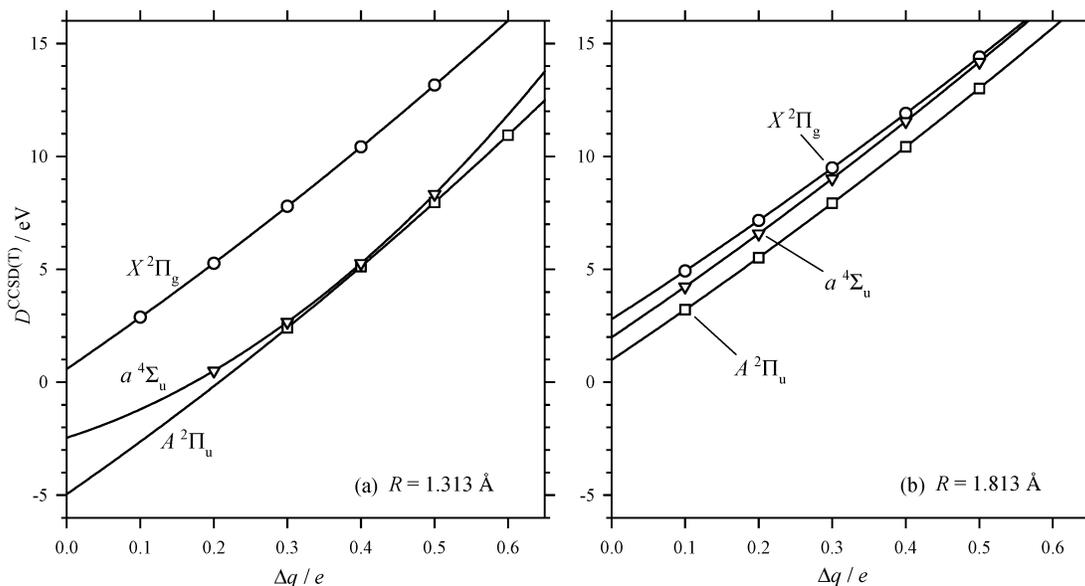
Figure 3. Representative plots of detachment energies vs Δq (incremental charge on the oxygen nuclei) computed in the stabilization calculations showing quadratic fits for the extrapolation to $\Delta q = 0$. (a) $R = 1.313$ C (left) and (b) $R = 1.813$ C (right). Circles, O_2^- X $^2\Pi_g$; inverted triangles, O_2^- a $^4\Sigma_u^-$; squares, O_2^- A $^2\Pi_u$.
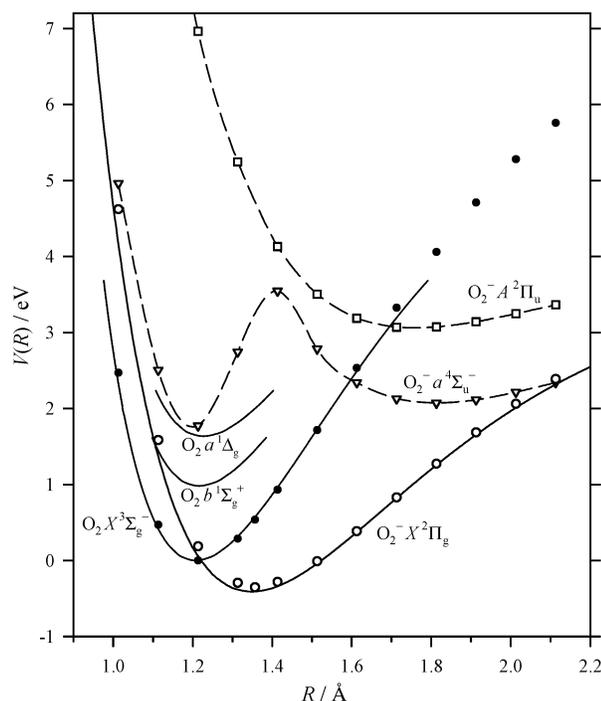
Figure 4. Calculated potential energies for O_2 X $^3\Sigma_g^-$ (solid circles), O_2^- X $^2\Pi_g$ (open circles), O_2^- a $^4\Sigma_u^-$ (inverted triangles), and O_2^- A $^2\Pi_u$ (squares). Solid lines are experimental RKR curves[68] for the neutral states and a Morse oscillator potential using the constants in Table 2 for the O_2^- X $^2\Pi_g$ ground-state anion. Dashed lines connect the calculated points of the anion excited states as a guide.

state, where it is metastable, are probably less reliable (i.e., 0.5 eV) than what we report for the X $^2\Pi_g$ and A $^2\Pi_u$ states.

After extrapolating the $D^{CCSD(T)}$ versus Δq values for each of the anion states at each of 13 R-values in the range 1.0–2.1 Å, we add the $D^{CCSD(T)}(\Delta q \rightarrow 0.0)$ data to the CCSD(T)/aug-cc-pVTZ computed ground-state neutral energies to produce potential curves for the anion states. The neutral and anion energy curves are shown in Figure 4, where we see that all three anion states have regions where they lie below the ground state of the neutral as well as regions where they lie above.

The electron affinity obtained at the CCSD(T)/aug-cc-pVTZ level is $EA_e(O_2) = 0.354$ eV, the O_2 X $^3\Sigma_g^-$ ← O_2^- X $^2\Pi_g$ difference between the two minima of the ground-state curves without vibrational zero-point energy (ZPE), spin–orbit, or other corrections. This result is in good agreement with the present experimental value of $EA_e(O_2) = 0.409$ eV from Table 2 (corrected from the observed 0 K value of $EA_0(O_2) = 0.448$ eV for O_2 X $^3\Sigma_g^-$ ← O_2^- X $^2\Pi_{3/2}$ for vibrational ZPE and spin–orbit splitting), an error of only 55 meV. The CCSD(T)/aug-cc-pVTZ value is sufficiently close to experiment to show that the potential curves shown in Figure 4 are of adequate quality to support the conclusions reached in this paper. Higher-order calculations are required to match the electron affinity within the experimental uncertainty. In a high-level coupled-cluster study of the ground states (but no excited states) of the neutral and anion, Neogrady et al.[50] reported a 0 K value of $EA_0(O_2) = 0.449 \pm 0.008$ eV, obtained by employing a comprehensive set of theoretical corrections including vibrational ZPE, core correlation, scalar relativistic effects, spin–orbit energy, and complete basis set extrapolation. Their value is in superb agreement with the experimental electron affinity.

The theoretical potential energy curves of Figure 4 definitively show that the O_2^- X $^2\Pi_g$ ground state is the only anion state with a minimum below the neutral ground-state minimum. The lowest anion excited states, O_2^- a $^4\Sigma_u^-$ and A $^2\Pi_u$, have shallow minima at much larger internuclear distances. These minima lie below the outer wall of the neutral ground-state potential curve, which suggests that these states could be metastable in low vibrational levels. However, their lifetimes are expected to be short if their vibrational wave functions extend to shorter R-values where they become electronically unstable. Although all of the O_2^- potentials correlating with $O(^3P) + O^-(^2P)$ lie below O_2 at large R, where they can be attractive because of the charge-induced-dipole potential, only the ground state and the a $^4\Sigma_u^-$ and A $^2\Pi_u$ excited states have been found to possess minima at bond lengths in the electronically bound region, that is, minima that lie below the ground-state O_2 potential curve.

Figure 4 also compares the ab initio theoretical potential energy curves with potential curves generated from experimental data. The experimental curves for the low-lying neutral states of O_2 (X $^3\Sigma_g^-$, a $^1\Delta_g$, b $^1\Sigma_g^+$) are spectroscopic RKR curves

TABLE 5: Calculated Molecular Constants for O_2^-

species	value	exp	CCSD(T)	MR-CI	MC-SCF	valence CI	MC-SCF	CCSD(T)	MR-CI	QCISD(T)	CCSD(T)	MR-CI
O_2 X$^3\Sigma_g^-$	EA_0/eV	0.448 ± 0.006							0.389		0.449 ± 0.008	0.39
	EA_e/eV	0.409 ± 0.006	0.354		−0.37		0.403			0.373	0.418	
O_2^- X$^2\Pi_g$	T_e/eV	0	0	0	0	0	0	0	0	0		0
	r_e/Å	1.348 ± 0.008	1.356	1.373	1.35	1.34	1.33	1.348	1.362	1.357		1.364
	ω_e/cm^{-1}	1108 ± 20	1112	1065	1163	1089	1499	1132	1107	1108		1103
O_2^- a$^4\Sigma_u^-$	T_e/eV		2.40		2.79	2.05						
	r_e/Å		1.808		1.846	1.88	1.9					
	ω_e/cm^{-1}		569		572	605						
O_2^- A$^2\Pi_u$	T_e/eV		3.39	3.10	3.54	2.93						
	r_e/Å		1.758	1.805	1.743	1.92	1.6−1.9					
	ω_e/cm^{-1}		557	535	604	452						
	ref	this work	this work	55	40	56	57	53	50	54	51	52

from the review by Krupenie.[67] The anion ground-state curve is a Morse potential using the experimental constants in Table 2, shifted by $EA_e(O_2)$ relative to the O_2 X $^3\Sigma_g^-$ minimum. Very good agreement between experiment and theory is observed for the ground-state neutral and anion ground-state curves although differences begin to appear for the neutral at distances beyond ca. 1.8 Å. These differences arise because the unrestricted Hartree−Fock reference function used as a zeroth-order approximation to the coupled-cluster wave function has difficulty accurately treating the cleavage of the bond in this case. However, the ground-state anion curve agrees well with the Morse curve for the anion, so there is no reason to believe that the anion curves are in substantial error. Moreover, the three anion curves are very similar to those obtained by Tellinghuisen et al.[40] in regions where the anion states are electronically stable.

In Table 5, we collect parameters characterizing the minima on the anion potential curves shown in Figure 4 as well as corresponding values obtained by earlier workers.[40,51,53−57] The most useful comparisons are to recent multireference configuration interaction (MR−CI) calculations by Bruna and Grein[55] and multiconfiguration self-consistent field (MC−SCF) calculations by Ewig and Tellinghuisen,[40] because both studies examined the neutral and the ground and excited state potentials of the anion. The results obtained from our ab initio calculations are generally similar to those obtained by these earlier workers in the electronically bound regions, thereby further supporting our conclusions.

In contrast to previous work, our calculations are designed to continue the anionic potential energy curves into regions where they describe electronically unstable states. By carrying out stabilization calculations, we are able to calculate the O_2^- X $^2\Pi_g$ state for $R < 1.2$ Å and the a $^4\Sigma_u^-$ and A $^2\Pi_u$ states for $R \lesssim 1.6$ Å. We find that, although the O_2^- X $^2\Pi_g$ and A $^2\Pi_u$ states are repulsive at smaller R, the O_2^-a $^4\Sigma_u^-$ state has a secondary minimum near 1.2 Å not observed previously. This state likely has a very short lifetime with respect to electron detachment in this range of internuclear distances, so its Heisenberg width may render detection of such a minimum experimentally impossible. The origin of this inner minimum lies in an avoided crossing between a valence $(2p\pi_g)^2(2p\sigma_u)^1$ configuration and a Rydberg-like $(2p\pi_g)^2(np\sigma_u)^1$ configuration ($n > 2$). As a result of this avoided crossing, the nature of the singly occupied σ_u^* orbital changes as shown in Figure 5 from valencelike at larger R to Rydberg-like at shorter R. An analogous valence−Rydberg avoided crossing is seen in the corresponding $^4\Sigma$ state of the isoelectronic FO molecule.[99] To check the reliability of the stabilization calculations in the region with Rydberg-like character, we added additional Rydberg-like basis functions to the aug-cc-pVTZ basis (three diffuse s and three p functions) and repeated the calculations of the a $^4\Sigma_u^-$

R=1.113 Å   R=1.213 Å   R=1.413 Å

R=1.613 Å   R=2.013 Å
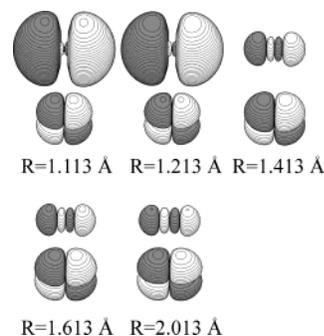
Figure 5. Molecular orbital plots for the $p\pi_g^*$ (bottom) and $p\sigma_u^*$ (top) orbitals of the O_2^- a $^4\Sigma_u^-$ state. The character of the $p\sigma_u^*$ antibonding orbital changes from valence (2p) at the outer minimum of the potential energy curve near 1.8 Å to Rydberg-like (np, $n > 2$) at the inner minimum near 1.2 Å.

state near the inner minimum. Although the energies change somewhat, as expected with a larger basis set, the general shape of the inner minimum is the same and the minimum remains at 1.2 Å.

Conclusions

The electron affinity of O_2 is firmly established by photoelectron spectroscopy as $EA_0 = 0.448 \pm 0.006$ eV. Although high-resolution rovibrational spectroscopy on O_2^- could improve the precision of the molecular constants of the X $^2\Pi_g$ ground state, its binding energy is quite well characterized by photoelectron spectroscopy, electron scattering, photodissociation, and collision-induced dissociation experiments. Theoretical coupled-cluster calculations and experimental evidence show that the ground X $^2\Pi_g$ state of O_2^- is the only electronic state below the $v' = 0$ level of the O_2 X $^3\Sigma_g^-$ neutral ground state. The lowest excited states of O_2^-, a $^4\Sigma_u^-$ and A $^2\Pi_u$, lie well above the adiabatic electron detachment limit for formation of O_2. The anion excited-state energies are predicted by theory to be $T_e($a $^4\Sigma_u^-) - T_e($X $^2\Pi_g) = 2.40$ eV and $T_e($A $^2\Pi_u) - T_e($X $^2\Pi_g) = 3.39$ eV at the CCSD(T)/aug-cc-pVTZ level. By employing stabilization methods, all three states of the anion have also been characterized at internuclear distances where they are unstable with respect to electron detachment. The stabilization calculations predict that the O_2^- a $^4\Sigma_u^-$ state has a secondary minimum near $R = 1.2$ Å as well as the minimum found by early workers at longer R.

Recent reports by Chen et al.[41−43] using the electron-capture detector (ECD) method, which is based on the temperature-dependent kinetics of electron attachment at atmospheric total pressure, give $EA(O_2) = 1.07 \pm 0.07$ eV and a doublet−quartet electronic excitation energy of 0.12 eV. These values are well outside any reasonable interpretation of modern spectroscopic,

8528 *J. Phys. Chem. A, Vol. 107, No. 41, 2003*

Ervin et al.

electron scattering, thermochemical, and ab initio theoretical data. This result carries the unequivocal implication that the ECD method is unable to provide accurate electron affinities and anion excited-state energies for O_2, a well-characterized diatomic molecule. A fundamental limitation of the ECD experiments[41−43] is that the ions responsible for the loss of electron current signal are not positively identified. Salyards et al.[100] have demonstrated that anions in atmospheric pressure systems with detachment energies less than about 0.8 eV are rapidly converted to $O_2^-(H_2O)$ clusters via fast reactions involving trace amounts of O_2 and H_2O. In the absence of spectroscopic or mass-spectrometric identification of the negative ions responsible for the electron-capture signals, the ECD method is evidently unreliable for determining electron affinities. The three different (outside the uncertainty limits) adiabatic electron affinities reported from analyses of ECD measurements by Chen et al., EA(O_2) = 0.46 ± 0.05 eV in 1983,[23] 0.9 ± 0.05 eV in 2002,[41] and 1.07 ± 0.07 eV in 2002−3,[42,43] further suggest the unreliability of ECD. Of the 12 electronic states of O_2^- proposed by Chen and Chen[43] to lie below the O_2 + e$^-$ detachment limit, only the X $^2\Pi_g$ ground state is actually thermodynamically stable with respect to electron detachment. The proposed reassignments of the origin band in the photo-electron spectra of O_2^- to either $^4\Sigma_{u(1/2)}^-$ and $^4\Sigma_{u(3/2)}^-$ (as given by Chen et al.[41]) or to $^2\Pi_{u(1/2)}$ and $^2\Pi_{u(3/2)}$ (as later reassigned by Chen and Chen[43]), as well as reassignments of vibrational transitions to additional anion electronic states,[43] have no basis in experiment or theory. Substantial revision of a well-established thermochemical quantity such as the electron affinity of O_2 would require very strong experimental evidence, which is not provided by the ECD measurements. Similar conclusions apply to the large revision of EA(NO) proposed by Chen et al.[41] to 0.85 eV from the photoelectron spectroscopy value[12] of EA$_0$(NO) = 0.026 ± 0.005 eV. While the detailed analyses and conclusions presented here apply specifically to the superoxide ion, the clear implication is that all electron-capture detector measurements of electron affinities should be considered subject to large and unknown errors.

References and Notes

(1) Ferguson, E. E.; Arnold, F. *Acc. Chem. Res.* **1981**, *14*, 327.

(2) Prabhakar, R.; Siegbahn, P. E. M.; Minaev, B. F.; Cgren, H. *J. Phys. Chem. B* **2002**, *106*, 3742.

(3) Bartmess, J. E. In *NIST Chemistry WebBook, NIST Standard Reference Database Number 69*; Mallard, W. G., Linstrom, P. J., Eds.; National Institute of Standards and Technology: Gaithersburg, MD, March 2003 (http://webbook.nist.gov/chemistry/, accessed 6/1/2003).

(4) Bailey, T. L.; Mahadevan, P. *J. Chem. Phys.* **1970**, *52*, 179.

(5) Vogt, D.; Hauffle, B.; Neuert, H. *Z. Phys.* **1970**, *232*, 439.

(6) Stockdale, J. A. D.; Compton, R. N.; Hurst, G. S.; Reinhardt, P. W. *J. Chem. Phys.* **1969**, *50*, 2176.

(7) Pack, J. L.; Phelps, A. V. *J. Chem. Phys.* **1966**, *44*, 1870.

(8) Phelps, A. V.; Pack, J. L. *Phys. Rev. Lett.* **1961**, *6*, 111.

(9) Burch, D. S.; Smith, S. J.; Branscomb, L. M. *Phys. Rev.* **1958**, *112*, 171.

(10) Celotta, R. J.; Bennett, R. A.; Hall, J. L.; Siegel, M. W.; Levine, J. *Phys. Rev. A* **1972**, *6*, 631. Reported value of EA(O_2) = 0.440 ± 0.008 eV corrected to 0.436 ± 0.008 eV to account for revision in EA(O) from 1.465 eV used in the electron energy calibration to the current value of 1.46111 eV.

(11) Corderman, R. R.; Engelking, P. C.; Lineberger, W. C. *Appl. Phys. Lett.* **1980**, *36*, 533.

(12) Travers, M. J.; Cowles, D. C.; Ellison, G. B. *Chem. Phys. Lett.* **1989**, *164*, 449.

(13) Posie, L. A.; Deluca, M. J.; Johnson, M. A. *Chem. Phys. Lett.* **1986**, *1986*, 170.

(14) Lavrich, D. J.; Buntine, M. A.; Serxner, D.; Johnson, M. A. *J. Chem. Phys.* **1993**, *99*, 5910.

(15) Buntine, M. A.; Lavrich, D. J.; Dessent, C. E.; Scarton, M. G.; Johnson, M. A. *Chem. Phys. Lett.* **1993**, *216*, 471.

(16) Bailey, C. G.; Lavrich, D. J.; Serxner, D.; Johnson, M. A. *J. Chem. Phys.* **1996**, *105*, 1807.

(17) Ervin, K. M.; Lineberger, W. C. In *Advances in Gas Phase Ion Chemistry*; Adams, N. G., Babcock, L. M., Eds.; JAI: Greenwich, CT, 1992; Vol. 1, p 121.

(18) Hanold, K. A.; Sherwood, C. R.; Garner, M. C.; Continetti, R. E. *Rev. Sci. Instrum.* **1995**, *66*, 5507.

(19) Schiedt, J.; Weinkauf, R. *Z. Naturforsch. A* **1995**, *50*, 1041.

(20) Boesl, U.; Bässmann, C.; Käsmeier, R. *Int. J. Mass Spectrom.* **2001**, *206*, 231.

(21) Allan, M. *J. Phys. B: At. Mol. Opt. Phys.* **1995**, *28*, 5163.

(22) Stephen, T. M.; Burrow, P. D. *J. Phys. B: At. Mol. Phys.* **1986**, *19*, 3167.

(23) Chen, E. C. M.; Wentworth, W. E. *J. Phys. Chem.* **1983**, *87*, 45.

(24) Tiernan, T. O.; Wu, R. L. C. *Adv. Mass Spectrom.* **1978**, *7A*, 136.

(25) Durup, M.; Parlant, G.; Appell, J.; Durup, J.; Ozenne, J.-B. *Chem. Phys.* **1977**, *25*, 245.

(26) Burrow, P. D. *Chem. Phys. Lett.* **1974**, *26*, 265.

(27) Baede, A. P. M. *Physica* **1972**, *59*, 541.

(28) Van de Wiel, H.; Tommassen, P. *J. Chromatogr.* **1972**, *71*, 107.

(29) Tiernan, T. O.; Hughes, B. M.; Lifschitz, C. *J. Chem. Phys.* **1971**, *55*, 5692.

(30) Berkowitz, J.; Chupka, W. A.; Gutman, D. *J. Chem. Phys.* **1971**, *55*, 2733.

(31) Chantry, P. J. *J. Chem. Phys.* **1971**, *55*, 2746.

(32) Nalley, S. J.; Compton, R. N. *Chem. Phys. Lett.* **1971**, *9*, 529.

(33) Lacmann, K.; Herschbach, D. R. *Chem. Phys. Lett* **1970**, *6*, 106.

(34) Ikezawa, M.; Rolfe, J. *J. Chem. Phys.* **1973**, *58*, 2024.

(35) Rolfe, J. *J. Chem. Phys.* **1979**, *70*, 2463.

(36) Van Brunt, R. J.; Kieffer, L. J. *Phys. Rev. A* **1970**, *2*, 1899.

(37) Noble, C. J.; Higgins, K.; Wöste, G.; Duddy, P.; Burke, P. G.; Teubner, P. J. O.; Middleton, A. G.; Brunger, M. J. *Phys. Rev. Lett.* **1996**, *76*, 3534.

(38) Brunger, M. J.; Middleton, A. G.; Teubner, P. J. O. *Phys. Rev. A* **1998**, *57*, 208.

(39) van Leeuwen, P. A.; Vreeker, R.; Glasbeek, M. *Phys. Rev. B* **1986**, *34*, 3483.

(40) Ewig, C. S.; Tellinghuisen, J. *J. Chem. Phys.* **1991**, *95*, 1097.

(41) Chen, E. S.; Wentworth, W. E.; Chen, E. C. M. *J. Mol. Struct.* **2002**, *606*, 1.

(42) Chen, E. S.; Chen, E. C. M. *J. Phys. Chem. A* **2002**, *2002*, 6665.

(43) Chen, E. S.; Chen, E. C. M. *J. Phys. Chem. A* **2003**, *107*, 169.

(44) Field, D.; Mrotzek, G.; Knight, D. W.; Lunt, S.; Ziesel, J. P. *J. Phys. B: At. Mol. Opt. Phys.* **1988**, *21*, 171.

(45) Spence, D.; Schulz, G. J. *Phys. Rev. A* **1970**, *2*, 1802.

(46) Linder, F.; Schmidt, H. *Z. Naturforsch. A* **1971**, *26*, 1617.

(47) Gray, R. L.; Haselton, H. H.; Krause, D., Jr.; Soltysik, E. A. *Chem. Phys. Lett.* **1972**, *13*, 51.

(48) Land, J. E.; Raith, W. *Phys. Rev. A* **1974**, *9*, 1592.

(49) Ziesel, J.-P.; Randell, J.; Field, D.; Lunt, S. L.; Mrotzek, G.; Martin, P. *J. Phys. B: At. Mol. Opt. Phys.* **1993**, *26*, 527.

(50) González-Luque, R.; Merchán, M.; Fülscher, M. P.; Roos, B. O. *Chem. Phys. Lett.* **1993**, *204*, 323.

(51) Neogrády, P.; Medved, M.; Černušák, I.; Urban, M. *Mol. Phys.* **2002**, *100*, 541.

(52) Stampfuss, P.; Wenzel, W. *Chem. Phys. Lett.* **2003**, *370*, 478.

(53) Sordo, J. A. *J. Chem. Phys.* **2001**, *114*, 1974.

(54) Chandrasekher, C. A.; Griffith, K. S.; Gellene, G. I. *Int. J. Quantum Chem.* **1996**, *58*, 29.

(55) Bruna, P. J.; Grein, F. *Mol. Phys.* **1999**, *97*, 321.

(56) Michels, H. H. *Adv. Chem. Phys.* **1981**, *445*, 225.

(57) Krauss, M.; Neumann, D.; Wahl, A. C.; Das, G.; Zemke, W. *Phys. Rev. A* **1973**, *7*, 69.

(58) Leopold, D. G.; Murray, K. K.; Stevens Miller, A. E.; Lineberger, W. C. *J. Chem. Phys.* **1985**, *83*, 4849.

(59) Ervin, K. M.; Ho, J.; Lineberger, W. C. *J. Chem. Phys.* **1989**, *91*, 5974.

(60) Neumark, D. M.; Lykke, K. R.; Andersen, T.; Lineberger, W. C. *Phys. Rev. A* **1985**, *32*, 1890.

(61) Andersen, T.; Haugen, H. K.; Hotop, H. *J. Phys. Chem. Ref. Data* **1999**, *28*, 1511.

(62) Blondel, C. *Phys. Scr.* **1995**, *T58*, 31.

(63) Valli, C.; Blondel, C.; Delsart, C. *Phys. Rev. A* **1999**, *59*, 3809.

(64) Slater, J.; Lineberger, W. C. *Phys. Rev. A* **1977**, *15*, 2277.

The Only Stable State of O_2^- Is X $^2\Pi_g$

J. Phys. Chem. A, Vol. 107, No. 41, 2003 **8529**

(65) Kelleher, D. E.; Martin, W. C.; Wiese, W. L.; Sugar, J. R.; Fuhr, K.; Olsen, A.; Musgrove, A.; Mohr, P. J.; Reader, J.; Dalton, G. R. *Phys. Scr. A* **1999**, *T83*, 158 (http://physics.nist.gov/asd, accessed 6/1/2003).

(66) Ervin, K. M. *PESCAL*; Fortran program, 2003.

(67) Engelking, P. C.; Lineberger, W. C. *Phys. Rev. A* **1979**, *19*, 149.

(68) Krupenie, P. H. *J. Phys. Chem. Ref. Data* **1972**, *1*, 423.

(69) Cheung, A. S.-C.; Yoshino, K.; Esmond, J. R.; Parkinson, W. H. *J. Mol. Spectrosc.* **1996**, *178*, 66.

(70) Herzberg, L.; Herzberg, G. *Astrophys. J.* **1947**, *105*, 353.

(71) Babcock, H. D.; Herzberg, L. *Astrophys. J.* **1947**, *108*, 167.

(72) Nieh, J.-C.; Valentini, J. J. *J. Phys. Chem.* **1987**, *91*, 1370.

(73) O'Brien, L. C.; Cao, H.; O'Brien, J. J. *J. Mol. Spectrosc.* **2001**, *207*, 99.

(74) Fiquet-Fayard, F. *J. Phys. B: At. Mol. Phys.* **1975**, *8*, 2880.

(75) Holzer, W.; Murphy, W. F.; Bernstein, H. J.; Rolfe, J. *J. Mol. Spectrosc.* **1968**, *26*, 543.

(76) Ervin, K. M.; Ramond, T. M.; Davico, G. E.; Schwartz, R. L.; Casey, S. M.; Lineberger, W. C. *J. Phys. Chem. A* **2001**, *105*, 10822.

(77) Halmann, M.; Laulicht, I. *J. Chem. Phys.* **1965**, *43*, 438.

(78) Engler, C. *Z. Phys. Chem. (Leipzig)* **1984**, *6*, 1193.

(79) Ho, J.; Ervin, K. M.; Lineberger, W. C. *J. Chem. Phys.* **1990**, *93*, 6987.

(80) Miller, C. E.; Drouin, B. J. *J. Mol. Spectrosc.* **2001**, *205*, 312.

(81) Cormack, A. J.; Yencha, A. J.; Donovan, R. J.; Lawley, K. P.; Hopkirk, A.; King, G. C. *Chem. Phys.* **1996**, *213*, 439.

(82) Tan, X. *Diatomic: A Spectral Simulation Program for Diatomic Molecules on Windows Platforms*, version 1.02 2002 (http://cs.jhu.edu/~xftan/Diatomic.html, accessed 6/1/2003).

(83) Gilles, M. K.; Polak, M. L.; Lineberger, W. C. *J. Chem. Phys.* **1992**, *96*, 8012.

(84) Taylor, B. N.; Kuyatt, C. *Guidelines for Evaluating and Expressing the Uncertainty of NIST Measurement Results*; NIST Technical Note 1297; National Institute of Standards and Technology: Washington, DC, 1994 (http://physics.nist.gov/Document/tn1297.pdf, accessed 6/1/2003).

(85) Gurvich, L. V.; Veyts, I. V.; Alcock, C. B. *Thermodynamic Properties of Individual Substances*, 4th ed.; Vol. 1 (Elements O, H (D, T), F, Cl, Br, I, He, Ne, Ar, Kr, Xe, Rn, S, N, P and Their Compounds), Parts 1-2; Hemisphere Publishing Corporation: New York, 1989.

(86) Ervin, K. M. *Chem. Rev.* **2001**, *101*, 391. Erratum, *Chem. Rev.* **2002**, *102*, 855.

(87) Cosby, P. C.; Huestis, D. L. *J. Chem. Phys.* **1992**, *97*, 6108.

(88) Simons, J.; Skurski, P. In *Theoretical Proscpect of Negative Ions*; Kalcher, J., Ed.; Research Signpost: Trevandrum, India, 2002; p 117.

(89) Simons, J. In *Encyclopedia of Chemical Physics and Physical Chemistry*; Moore, J., Spencer, N., Eds.; Institute of Physics: Philadelphia, PA, 2001; p 1907.

(90) Botschwina, P.; Seeger, S.; Mladenović, M.; Schulz, B.; Horn, M.; Schmatz, S.; Flügge, J.; Oswald, R. *Int. Rev. Phys. Chem.* **1995**, *14*, 169.

(91) Kalcher, J.; Sax, A. F. *Chem. Rev.* **1994**, *94*, 2291.

(92) Taylor, H. S. *Adv. Chem. Phys.* **1970**, *18*, 91.

(93) Simons, J. *J. Chem. Phys.* **1981**, *75*, 2465.

(94) Simons, J. In *Resonances in Electron−Molecule Scattering, Van Der Waals Complexes, and Reactive Chemical Dynamics*; ACS Symposium Series, No. 263; American Chemical Society: Washington, DC, 1984; pp 3−16.

(95) Simons, J. *J. Chem. Phys.* **1986**, *84*, 4462.

(96) Purvis, G. D., III; Bartlett, R. J. *J. Chem. Phys.* **1982**, *76*, 1910.

(97) Kendall, R. A.; Dunning, T. H., Jr.; Harrison, R. J. *J. Chem. Phys.* **1992**, *96*, 6792.

(98) Frisch, M. J.; Trucks, G. W.; Schlegel, H. B.; Scuseria, G. E.; Robb, M. A.; Cheeseman, J. R.; Zakrzewski, V. G.; Montgomery, J. A., Jr.; Stratmann, R. E.; Burant, J. C.; Dapprich, S.; Millam, J. M.; Daniels, A. D.; Kudin, K. N.; Strain, M. C.; Farkas, O.; Tomasi, J.; Barone, V.; Cossi, M.; Cammi, R.; Mennucci, B.; Pomelli, C.; Adamo, C.; Clifford, S.; Ochterski, J.; Petersson, G. A.; Ayala, P. Y.; Cui, Q.; Morokuma, K.; Malick, D. K.; Rabuck, A. D.; Raghavachari, K.; Foresman, J. B.; Cioslowski, J.; Ortiz, J. V.; Baboul, A. G.; Stefanov, B. B.; Liu, G.; Liashenko, A.; Piskorz, P.; Komaromi, I.; Gomperts, R.; Martin, R. L.; Fox, D. J.; Keith, T.; Al-Laham, M. A.; Peng, C. Y.; Nanayakkara, A.; Gonzalez, C.; Challacombe, M.; Gill, P. M. W.; Johnson, B.; Chen, W.; Wong, M. W.; Andres, J. L.; Gonzalez, C.; Head-Gordon, M.; Replogle, E. S.; Pople, J. A. *Gaussian98*, Revision A.7; Gaussian, Inc.: Pittsburgh, PA, 1998.

(99) Lane, I. C.; Orr-Ewing, A. J. *J. Phys Chem. A* **2000**, *104*, 8759.

(100) Salyards, M. J.; Knighton, W. B.; Grimsrud, E. P. *Int. J. Mass Spectrom.* **2003**, *222*, 201.